Title: Reactive oxygen species drive downward vertical migration in diatom microphytobenthic biofilms as a strategy to cope with oxidative stress

Short title: ROS-Driven Diatom Biofilm Migration

Authors informations:

1. Alexandre Desparmet[1] (alexandre.desparmet@mnhn.fr ; ORCID 0009-0009-6783-277X)
2. Bruno Jesus[2] (bruno.jesus@univ-nantes.fr ; ORCID 0000-0002-2047-3783)
3. Tony Robinet[1] (tony.robinet@mnhn.fr ; ORCID 0000-0002-3669-2788)
4. Thierry Dufour[3] (thierry.dufour@sorbonne-universite.fr ; ORCID 0000-0002-0397-368X)
5. Cédric Hubas[1] (cedric.hubas@mnhn.fr ; ORCID 0000-0002-9110-9292)

[1]Laboratoire de Biologie des Organismes et Écosystèmes Aquatiques (BOREA), UMR 8067, Muséum National d'Histoire Naturelle, Sorbonne Université, CNRS 7208, IRD 207, UCN, UA, Station Marine de Concarneau, Quai de la Croix, 29900 Concarneau, France.

[2]Institut Des Substances et Organismes de la Mer (ISOMer), UR 2160, Nantes université, Faculté des Sciences et des Techniques, 44000 Nantes, France.

[3]Laboratoire de Physique des plasmas (LPP), UMR 7648, Sorbonne Université, CNRS, École Polytechnique, Univ. Paris-Sud, Observatoire de Paris, Université Paris-Saclay, PSL Research University, 4 Place Jussieu, 75252 Paris, France.

Corresponding author:

Alexandre Desparmet
Laboratoire de Biologie des Organismes et Écosystèmes Aquatiques (BOREA), UMR 8067, Muséum National d'Histoire Naturelle, Sorbonne Université, CNRS 7208, IRD 207, UCN, UA, Station Marine de Concarneau, Quai de la Croix, 29900 Concarneau, France.
alexandre.desparmet@mnhn.fr ; ORCID 0009-0009-6783-277X

ABSTRACT

Diatom-dominated intertidal microphytobenthic biofilms experience daily fluctuations in irradiance, which can lead to oxidative stress within the photosynthetic apparatus through the production and accumulation of reactive oxygen species. To maintain photosynthetic efficiency, benthic diatoms have developed protective strategies, including the mobilization of antioxidant xanthophyll cycle and the ability for vertical migration through the sediment. However, the cellular signaling pathways underlying migration remain poorly characterized. This study investigated the triggering effect of reactive oxygen species on behavioral and photophysiological responses, through the analysis of lipophilic pigments and fluorescence parameters. To this end, two microphytobenthic communities, one with sediment allowing vertical migration and another without sediment restricting it, were exposed to irradiance, cold atmospheric plasma, and hydrogen peroxide stresses. Results showed a consistent downward migration response under all oxidative stresses, highlighting the key role of reactive oxygen species, especially hydrogen peroxide, in triggering and driving this microphytobenthic behavior. Moreover, a difference was observed between the pathways involved in vertical migration and those underlying the photophysiological response. Hydrogen peroxide and cold atmospheric plasma stresses highlighted the necessity of substantial microphytobenthic migration, whereas irradiance induced a specific and controlled response involving engagement of the xanthophyll cycles, acting in synergy with the migration strategy by showing stronger activation when migration was impaired. By establishing that the rapid and efficient migration strategy, acting in synergy with xanthophyll cycles in epipelic cells, is induced by reactive oxygen species, this study provides key insights into the molecular basis of microphytobenthic responses to cellular and environmental oxidative stress.

Key Words : *Diatom microphytobenthic biofilms | Pleurosigma strigosum | Vertical migration | ROS | Light stress | Cold Atmospheric Plasma | Hydrogen peroxide | Xanthophyll cycles | Photophysiology*

Abbreviations : *Chlorophyll a, Chla; Diadinoxanthin, Dd; Diadinoxanthin-Diatoxanthin De-epoxidation state, D-DES; Diatoxanthin, Dt; Minimum very low light-adapted fluorescence yield,* F_0*; Light utilisation efficiency under light adapted state, Fq'/Fm'; High light, HL; Hydrogen peroxide, HP; Microphytobenthos, MPB; Maximum non-photochemical quenching at 1000 µmol photons.*$m^{-2}.s^{-1}$*,* NPQ^{1000}*; Cold atmospheric plasma, PL; Photosystem II, PSII; Maximum relative electrons transport rate observed,* $rETR_{m\ obs}$*; Reactive oxygen species, ROS; Sediment biofilm, SB; Xanthophyll cycle of Violaxanthin-Antheraxanthin-Zeaxanthin, VAZ; Very Low Light adapted control, VLL; Without sediment biofilm, WSB; Xanthophyll cycles, XC; Yield of non-regulated energy dissipation, Y(NO); Yield of regulated non-photochemical quenching, Y(NPQ); Violaxanthin-Antheraxanthin-Zeaxanthin De-epoxidation state, Z-DES.*

INTRODUCTION

The aquatic microbiome exhibits a remarkable diversity of adaptive strategies to deal with rapid environmental fluctuations. Intertidal sediments, as dynamic interfaces, undergo significant qualitative and quantitative variations in the electromagnetic spectrum throughout the day, impacting the phototrophic communities [1]. Among these, microphytobenthos (MPB), dominated by epipelic diatoms, forms a structured mucilaginous biofilms on muddy substrates, an advantageous lifestyle that plays a key role in its adaptation and associated ecosystem services [2–4].

Light carries essential environmental information that diatoms can perceive either directly through photoreceptors or indirectly *via* cellular signals, such as levels of reactive oxygen species (ROS) and the redox state of the photosynthetic chain, triggering physiological responses involved in light acclimation, photoprotection and photomotile movements, enabling diatoms to acclimate, adapt, and survive [5]. Under high light intensity conditions, photosynthetic capacity can be exceeded, leading to the synthesis and accumulation of ROS, natural by-products of oxygen metabolism, such as singlet oxygen $^1O_2$, superoxide $O_2^{\bullet-}$, hydrogen peroxide H_2O_2 and hydroxyl $HO^\bullet$ [6]. This deregulation leads to photooxidative damages, disrupting homeostasis, inducing lipid peroxidation that compromises cellular integrity [7], oxidizing DNA and key proteins such as the D1 protein of PSII [8, 9], and can ultimately result in cell death [6, 10]. Epipelic diatoms have developed two major adaptive strategies to pre-empt this ROS formation and accumulation, ensuring optimal photosynthetic processes in a variable light environment: vertical migration behavior and xanthophyll cycle (XC) [11, 12].

First described in 1907 by Fauvel and Bohn [13], the ability of cells to move vertically through muddy substrates is a photobehavior regulated both endogenously and plastically by various environmental forcing, such as light information [14–19]. Rapid and temporally adjustable, this actin-myosin-driven gliding system involving the secretion of extracellular mucilage fibrils through the slit raphe, enables diatoms to quickly reposition themselves at low metabolic cost, allowing them to reach sediment layers with optimal irradiance conditions [18, 20–22, 17, 23, 19, 24]. This adaptation, partly responsible for the diversity of Bacillariophyta [25], represents a significant evolutionary advantage and gave rise to distinct migration strategies depending on the context [12, 14, 16, 17]. In addition, the optimization of diatom light-harvesting, results from the accessory carotenoid pigment dynamic regulation, such as xanthophylls associated with the photosystem II Fucoxanthin-Chlorophyll-Protein supercore complex [11, 26–28]. Overstimulation of the photosynthetic electron transport chain leads to acidification of the thylakoid lumen due to the photolytic activity of photosystem II (PSII). Under these conditions of low lumen pH, the enzymatic activity of Diadinoxanthin de-epoxidase is

upregulated, leading to the de-epoxidation of Diadinoxanthin (Dd) embedded in the thylakoid membranes [12, 29]. Rapid XC adjustments involved in the energy-dependent component of non-photochemical quenching (qE) are particularly pronounced in diatoms and reflect a crucial antioxidant photoprotective response that optimizes thermal dispersion of excess energy in a fluctuating environment, limiting ROS-associated damage in the chloroplast [12, 27, 29, 30]. These two major adaptations are complemented by others, such as chloroplast mobility [31], spatial cell orientation [32, 33], frustule nanostructures [34], a wide variety of photoreceptors [35, 36], as well as cellular ROS management through enzymatic antioxidant capacities [37] and non-enzymatic pathways involving carotenoids, glutathione, vitamins such as ascorbic acid, or phenolic compounds like flavonoids [28, 38]. All these adaptations are part of a sophisticated system that enables diatoms to monitor and respond to environmental fluctuations, contributing to their success in modern marine ecosystems [39].

However, while both diatom vertical migration photo-regulation and XC are well characterized individually, the molecular ROS-related cellular signaling pathways that coordinate and integrate real-time protective strategies, remain poorly understood in benthic diatoms. The present study addresses this gap by testing the hypothesis that: (1) oxidative stress mediated by ROS is involved in triggering the vertical downward migration response; and (2) not all oxidative stress conditions are sufficient to induce a complete photophysiological response, in a natural epipelic microphytobenthic biofilm.

MATERIALS AND METHODS

BIOFILM SAMPLING AND EXPERIMENTAL CONDITIONS

MPB sampling. Microphytobenthos was collected from an outdoor disused breeding pond at the Concarneau Marine Station (France; 47°52’05.85”N; 3°55’00.51”W), which contain fine-grained muddy sediments exposed to a semi-diurnal tidal cycle (**Figure. 1A and C**). The upper centimeter of sediment was sampled at low tide on April 29, 2024 (1:00 PM), using a shovel. Samples were placed in plastic boxes, transported to the laboratory, and left to settle in darkness for 24 hours at 20°C.

Community groups. Two communities were compared: one capable of vertical migration through sediment (Sediment Biofilm, SB), and another with impaired vertical movement due to the absence of sediment (Without Sediment Biofilm, WSB). The latest was obtained by transferring the upper millimeter of the SB community, into filtered site seawater, using tweezers. For molecular

analyses, five replicate petri dishes (*n=5*) were prepared for each condition and stress, while three replicates (*n=3*) were used in photophysiological measurements.

Oxidative condition exposures. Both communities were exposed in the morning (9:00 AM to 1:00 PM) to three short oxidative stresses and compared to a Very Low Light (VLL ; below 5 µmol photons.m^{-2}.s^{-1}) adapted controls. High light (HL) stress was done, to mimic intense irradiance commonly experienced by autotrophic cells in natural environments, with a 30-minute exposure to 1500 µmol photons·m^{-2}·s^{-1} of full-spectrum warm white LED light panel (GR-RHINO-260-PRO-DIM, Rhino Series). A cold atmospheric plasma (PL) was applied for 10 minutes by piezoelectric discharge (PiezoBrush® PZ3, Relyon Plasma GmbH), using ambient laboratory air as the carrier gas. This treatment induces changes in temperature and pH, and generates reactive oxygen and nitrogen species, as characterized by Thompson et al, 2025 [40] (See supplementary materials), thereby simulating a composite environmental oxidative stress reflective of the complex surroundings of microphytobenthos. According to a spectrophotometric determination of H_2O_2 generated in plasma activated seawater, a third stress consisting of a 10-minute exposure to a 200 µM hydrogen peroxide (HP) solution (Sigma-Aldrich® ref. 216763) was applied in order to isolate the impact of this specific ROS. Both HP and PL exposures were applied under VLL.

METABARCODING APPROACH

MPB communities were characterized using a short-read Illumina® metabarcoding approach. DNA was extracted using the NucleoSpin® Soil Mini kit (MACHEREY-NAGEL®, ref. 740780.10). The V3-V4 region of the 16S rRNA gene was amplified using primers 338F [41] and 806R [42], and the V4 region of the 18S rRNA gene with primers TAReuk454FWD1 and TAReukREV3 [43]. Library construction and sequencing were performed by BMKGENE. Raw data were processed using the SAMBA workflow to generate amplicon sequence variants, assigned taxonomically with the PR2 (v5.0.0) database for eukaryotes and SILVA (v138.1) for prokaryotes.

CHLOROPHYLL FLUORESCENCE: PULSE AMPLITUDE MODULATED FLUOROMETRY

Photosynthetic parameters derived from chlorophyll *a* (Chla) fluorescence were measured using a MonitoringPen MP 100-E® (Photon System Instruments), with a light curve program consisting of seven one-minute irradiance steps, increasing from 10 to 1000 µmol photons.m^{-2}.s^{-1} ($\lambda_{LED\ ex}$ 470 nm). The initial linear slope Alpha (α) reflecting the maximum light use efficiency of PSII, was derived from rETR-irradiance curves by fitting the Eilers and Peeters (1988) model [44], modified by Silsbe and Kromkamp (2012) [45]. The maximum quantum yield of PSII photochemistry (Fq'/Fm'), the maximum

relative electron transport rate (rETR) used as a proxy for carbon fixation, the non-photochemical quenching (NPQ), and its partitioning into regulated Y(NPQ) and non-regulated Y(NO) components, were calculated using equations adapted from Consalvey et al. (2005) [46] (**Table S1**). Measurements were taken after a 10-minute VLL adaptation for HL, and after the 10-minute stress period for HP and PL, which were both performed under VLL.

The minimum fluorescence of VLL-adapted samples (F_0), used as a proxy for surface algal biomass, was monitored in the SB community under oxidative stress compared to VLL controls, to assess the vertical migratory response. Additionally, F_0 was tracked over a 14-day period, without any environmental signals, to characterize the biofilm endogenous vertical migration pattern.

LIPOPHILIC PIGMENTS ANALYSIS

Lipophilic pigments were extracted following the Brotas and Plante-Cuny, 2003 protocol [47]. Freeze-dried samples (10 mg WSB, 40 mg SB) were incubated 15 minutes at -21 °C in 2 mL of 95% methanol buffered with 2% ammonium acetate, then filtered through a 0.2 µm PTFE filter. Aliquots of 100 µL were injected into an Agilent 1260 Infinity HPLC system equipped with a C18 Supelcosil® column and a UV–VIS photodiode array detector (DAD 1260 VL, 250–900 nm). The method employed a flow rate of 0.6 $mL.min^{-1}$ using solvent mixture A (0.5 M ammonium acetate in 85:15 methanol:water), B (90:10 acetonitrile:water), and C (100% ethyl acetate). A total of 44 MPB pigments were detected (**Table. S2**), and their concentrations (µg of pigment.g of dry $weight^{-1}$) were quantified using calibration curves based on phytoplankton pigment standards from DHI®. Concentrations were expressed either as relative proportions or normalized to Σ_{Chla} (Chla and their derived forms), used as a biomass proxy (**see Fig. S1**). Two groups of derived Chla were identified. The "Chla-derivatives" group includes unidentified Chla-like pigments, as well as the allomer and epimer forms. The "Pheopigments" group includes Pheophytins *a*, Pheophorbides *a*, and Pyropheophytin *a*.

The ratios (%) of pigment concentrations normalized per Σ_{Chla} unit (µg), were determined from :

$$Ratio = \frac{[Pigment]}{[Chla] + [Chla{-}derivatives] + [Pheopigments]} \times 100 \quad \textbf{(1)}$$

The ratio between Dd and Diatoxanthin (Dt) concentrations (D-de epoxidation state, D-DES), was calculated as follows:

$$D\text{-}DES = \frac{[Diatoxanthin]}{[Diadinoxanthin] + [Diatoxanthin]} \times 100 \quad \textbf{(2)}$$

The ratio between Zeaxanthin, Antheraxanthin and Violaxanthin concentrations (Z- de epoxidation state, Z-DES), was determined as follows:

$$Z\text{-}DES = \frac{[Zeaxanthin]}{[Violaxanthin] + [Antheraxanthin] + [Zeaxanthin]} \times 100 \quad \textbf{(3)}$$

DATA TREATMENT

Raw metabarcoding data were processed using the SAMBA workflow. Reads were normalized by coverage-based rarefaction and transformed to relative abundances. Diversity between groups was tested using the Wilcoxon rank-sum test and community structure differences were assessed by MFA and ANOSIM on Euclidean distances. Circadian variation in MPB biomass was tested using a one-tailed Wilcoxon-Mann-Whitney test, and its correlation with the tidal cycle by a Spearman correlation. For both groups, the net impact values of stress $\Delta_{\text{After-Before}}$ on photophysiological parameters were calculated and compared to those of the VLL control, which accounts for metabolic drift over time, using Welch's two-sample t-test. Pigment composition was analyzed by PCA and ANOSIM to assess condition and group effects, SIMPER identified significant variations, and Between-Class Analysis characterized the stress impacts on dataset inertia. Changes in pigment ratios were tested using the Mann-Whitney U test.

RESULTS & DISCUSSION

MICROPHYTOBENTHIC COMMUNITY

Characterization of the MPB community using a metabarcoding approach (**Figure. 1D, E and Fig. S2**), provided a relevant semi-quantitative overview of dominant taxa and their relative abundances, despite inherent biases such as amplification of free environmental DNA and underrepresentation of rare species in communities [48]. Both groups showed distinct MPB assemblages (ANOSIM, R = 0.67; p-value = 1e-04) (**Fig. S3**), with a significantly lower pro- and eukaryotes diversity indices in the WSB (Wilcoxon-Mann-Whitney, p-value < 0.05) (**Fig. S4**). This result was expected given the sampling protocol, as WSB was derived from subsampling the surface SB layer, thereby excluding much of the sediment-associated diversity.

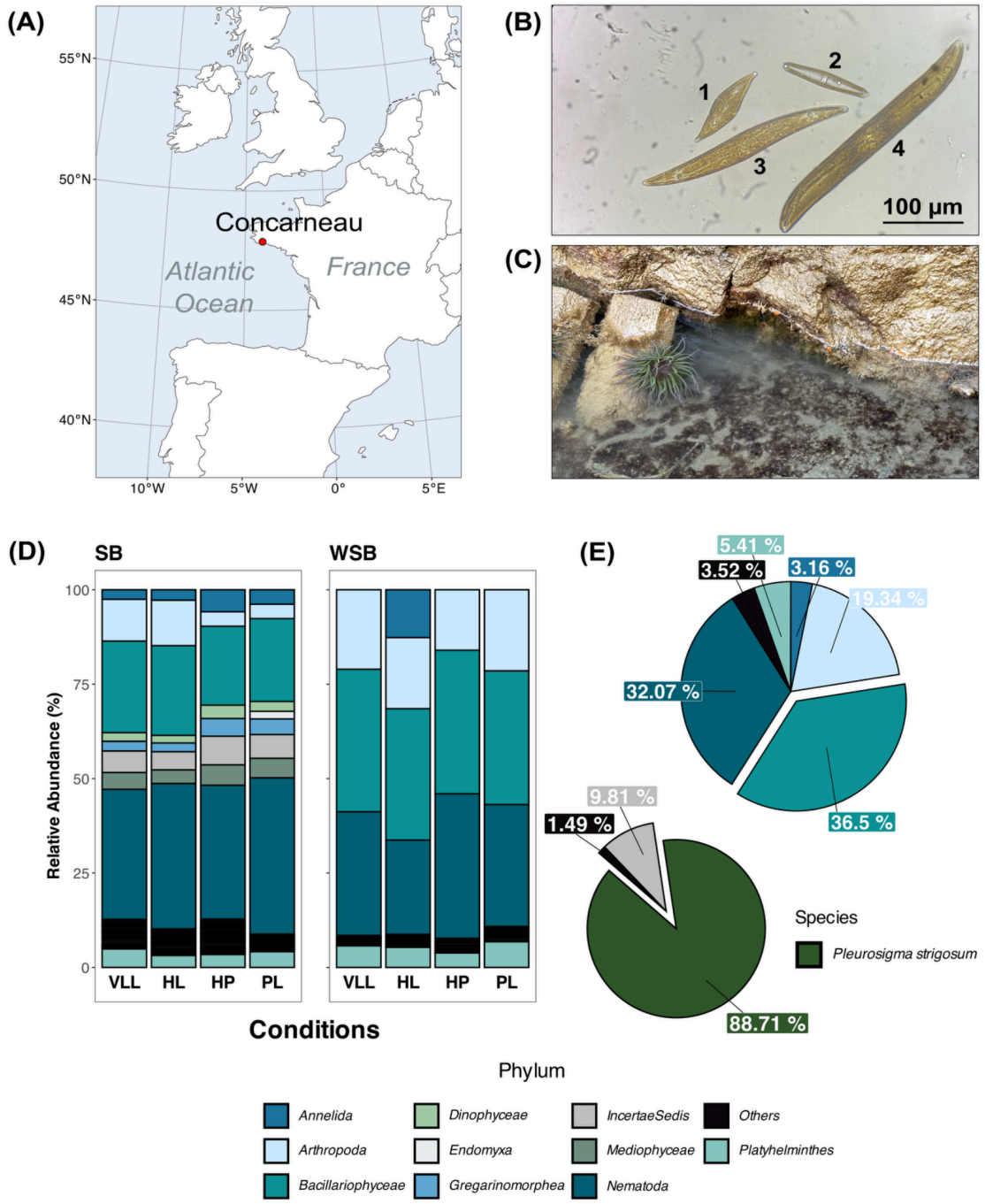

Figure 1. Microphytobenthic community diversity

(A) *Geographical location of the studied microphytobenthic biofilm.* ***(B)*** *Light microscopy image of the most commonly observed diatom species within the microphytobenthic community: 1. Pleurosigma sp., 2. Navicula sp., 3. Pleurosigma strigosum, 4. Gyrosigma sp.* ***(C)*** *Microphytobenthic biofilm (brown patches) developing on the muddy substrate of the breeding pond at the Concarneau Marine Station.* ***(D)*** *Relative average abundances barplot (%; n = 5 per condition) of microphytobenthic eukaryotic phyla. Very Low Light adapted control (VLL), High Light (HL), Hydrogen Peroxide (HP), and Cold Atmospheric Plasma (PL), for Sediment Biofilm (SB) and Without Sediment Biofilm (WSB) samples.* ***(E)*** *Average WSB microphytobenthic community across conditions, highlighting the prevalence of the autotrophic phylum Bacillariophyceae (first pie chart), and the notable*

contribution of Pleurosigma strigosum (second pie chart). The "Others" category includes taxa with <2% abundance.

Both eukaryotic community groups was represented by *Nematoda*, *Bacillariophyceae*, and *Arthropoda* with increased relative proportions of *Arthropoda* and *Bacillariophyceae* in WSB samples, along with a stabilizing effect on WSB community variability across replicates, due to subsampling (**Figure. 1D**). This eukaryotic MPB community composition corroborates microscopic observations [49] and literature on biofilms and meiofauna in similar environments, which consistently report the prevalence of nematodes, copepods, and ostracods in microphytobenthic biofilms [50, 51]. The autotrophic surface biovolume of MPB was largely dominated by the raphid species *Pleurosigma strigosum* accounting for 88.71% in WSB (**Figure. 1E**). This dominance of *Pleurosigma* was accompanied by other benthic diatoms (**Figure. 1B**), notably from the *Navicula* and *Gyrosigma* genera (possibly *G. balticum*, as suggested by Gaubert-Boussarie et al., 2020 [49]), although this diversity is likely underestimated due to the metabarcoding approach. Consistent with these findings, the observed behavioral, pigmentary, and photophysiological signals, can be largely attributed to the biovolume of the surface benthic diatoms, with *Pleurosigma strigosum* playing a predominant role.

VERTICAL MIGRATION BEHAVIOR IN SB GROUP

Endogenous migration. The linear relationship between F_0 and Chla concentration enables continuous monitoring of MPB biomass migratory behavior in the SB group throughout 14 days [14, 52]. MPB cells exhibited a robust and regular vertical migration behavior on a 23.6 hour period (**Figure S5.A and B**), driven by both endogenous circadian and tidal rhythms, with a significantly higher biomass accumulation at the sediment surface during daytime (one-tailed Wilcoxon-Mann-Whitney test, p-value < 0.05) and during neap tides (Spearman correlation = -0.65; p-value = 0.03; **Figure S5.C**). In MPB diatom biofilms, many biological processes are regulated endogenously, including the vertical migration behavior [16–18, 52]. However, a migration rhythm drift was observed at the end of the time series, with peaks of algal biomass occurring during nighttime (**Figure S5.A**). Although circadian rhythms are self-sustained in stramenopiles, the free-running signal requires regular resetting through light perception with specific photoreceptors, as phytochromes, or through red light perception itself, both seems playing a key role in synchronizing the circadian clock [53]. This endogenous behavior is also influenced by environmental factors [15], allowing for a rapid and temporally adjustable response [19, 21].

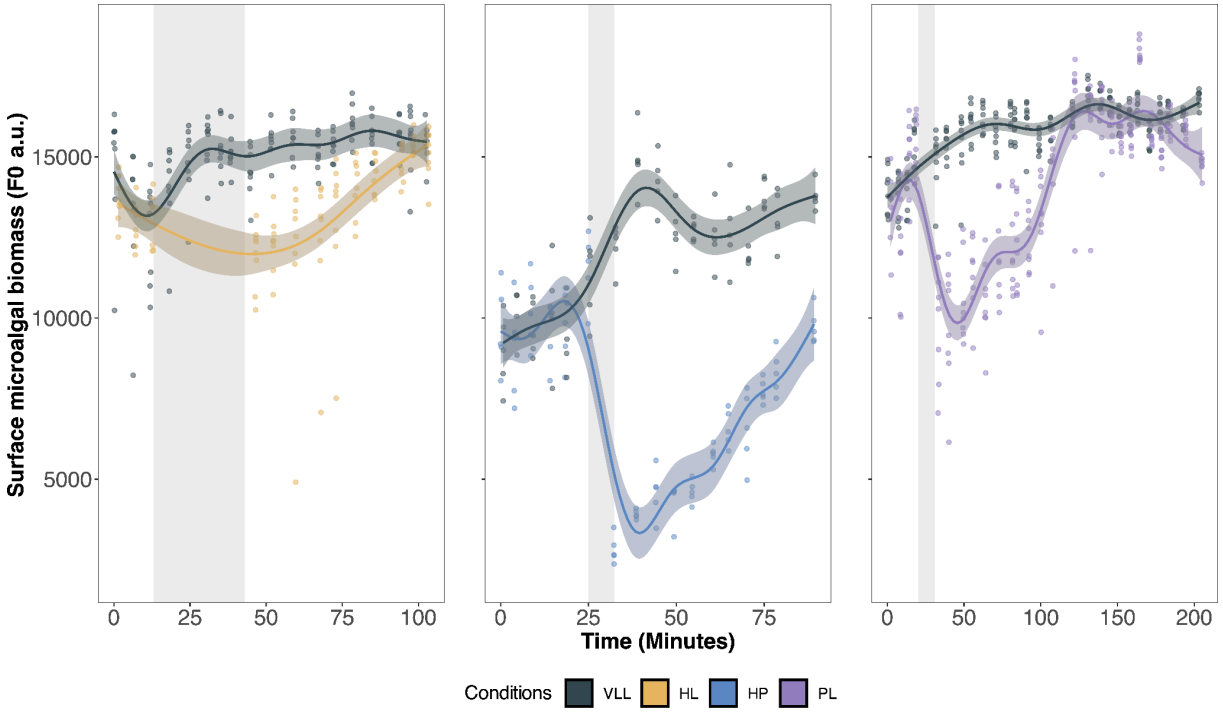

Figure 2. Downward migration of microphytobenthos under three oxidative stress

Temporal monitoring of surface microalgal biomass (F_0, arbitrary units) for the Sediment Biofilm (SB) sample group under three oxidative stress: High Light (HL) n = 8, Hydrogen Peroxide (HP) n = 5, and Cold Atmospheric Plasma (PL) n = 8, compared to a Very Low Light adapted control (VLL). Shaded grey areas correspond to the periods of stress application. All measurements are taken in the morning, during the upward migration phase of microphytobenthos.

Vertical motility under oxidative stress. The vertical migration response of SB samples was tested under three oxidative stresses. It is important to note that HP and PL-ROS stresses were exogenous (environmental ROS), in contrast to the endogenous ROS stress that occurred under irradiance conditions, even though HL-derived ROS from other cells are also actively and passively generated by diatoms and accumulate in the external environment surrounding them [10, 54]. Regardless of how ROS were generated and applied, the *P. strigosum*-dominated biofilms were able to sense both metabolic and environmental ROS and responded with a significant downward migration, followed shortly after the stress by a gradual surface biomass recovery, observed across all three stresses (**Figure. 2**).

Table 1. Extent of the behavioral response of the MPB surface biomass

Table of F_0 biomass changes (average ± SD) before and after (arbitrary units), at the sediment surface under oxidative stress compared to their respective Very Low Light adapted controls (VLL), for the Sediment Biofilm (SB) sample group (n = 8 for HL and PL; n = 5 for HP). The Δ After-Before (a.u.) and Changes (%) columns show the temporal evolution in surface F_0 After - Before stress, as shown in Figure. 2. The post-stress recovery slope is

calculated using a linear regression model applied to F_0 fluorescence kinetics over 60 minutes after stress cessation, as an indicator of MPB resilience. The slope reflects the rate of F_0 unit variation per minute during recovery ($F_0.min^{-1}$).

Conditions	F0 Before (a.u.)	F0 After (a.u.)	Δ After-Before (a.u.)	Changes (%)	Recovery slope (F0.min-1)
HL	13080 (807)	11916 (993)	-1164	**-9%**	**+67**
VLL (HL)	12752 (1606)	14540 (787)	+1788	**+14%**	**+11**
HP	11546 (1100)	2824 (433)	-8722	**-76%**	**+116**
VLL (HP)	11393 (1457)	12232 (703)	+839	**+7%**	**-2**
PL	15496 (843)	9979 (1801)	-5517	**-36%**	**+47**
VLL (PL)	15263 (726)	14906 (945)	-356	**-2%**	**+17**

Behavioral response intensity varied depending on stress type, with environmental ROS triggering the strongest effect, particularly HP, which induced a clear downward migration faster than the other stresses, occurring within approximately one minute (experimental observation). HP showed a drop of 75.5% in F_0, followed by PL with a 35.6% decrease, and HL associated with intracellular oxidative stress resulting in an 8.9% reduction (**Table. 1**). The migration behavior through a muddy substrate in response to HL stress is well documented in benthic diatoms [14, 18, 55, 56], including for *P. strigosum* [24], but is not exclusive to them, as it is also reported in other motile microorganisms under unfavorable irradiance, such as cyanobacteria, euglenoids, and other planktonic microalgae, highlighting a relatively common evolutionary advantage [14, 57, 58]. However, the findings also revealed that even brief exposure to HP and PL-generated ROS can trigger downward migration. The PL-induced response likely results from a synergy between stressors, as plasma generation leads to a composite environmental stress involving pH acidification, increased redox potential, and the production of a complex mix of UV radiation, free-radical and non-radical reactive oxygen and nitrogen species [40]. The significant role of ROS in triggering this behavior was supported by the HP-induced migration, which isolated the effect of H_2O_2 and highlighted its key role as a switch that initiates a strong, transient motile response, followed by rapid post-stress resilience in MPB. Hydrogen peroxide is naturally present in different sub-cellular compartments, has a relatively stable lifespan of up to several minutes, possesses a high oxidative potential, can cross membranes, is involved in cellular signal transduction, and is produced by microalgae under irradiance stress [6, 28].

ROS are capable of inducing other behavioral responses in microalgae, including the triggering of aggregation behavior observed in *Chlamydomonas reinhardtii* [59], or with a role of H_2O_2 in controlling motility in the microalgae *Euglena gracilis* and *Euglena agilis* following irradiance stress [60, 61], or even impacting the migratory behavior of phytoplankton cells in response to unfavorable environmental conditions [62]. Additionally, increased motility in benthic diatoms has been observed in response to abiotic stress induced by copper exposure, which affected cellular oxidative status,

cytoskeletal dynamics and the actin-myosin system [23]. In a broader context, ROS are frequently referenced in the literature as secondary messengers in various biological functions, both in animals and in terrestrial and aquatic autotrophs [6, 63], including diatoms [5, 64]. There is a synergy between responses to stress and ROS, such as H_2O_2, which handles the transduction of signals involved in adaptation to both biotic and abiotic environmental stresses by triggering defense mechanisms [38]. The cellular detection of key parameters, relies on a sophisticated signal transduction network to drive various physiological processes, including acclimation, photoprotection, and photomotile responses [5]. The establishment of the precise cellular pathway leading to this indirect photosensing behavior by the photosynthetic apparatus in benthic diatoms remains to be clarified in further investigation.

A better understanding of the signaling cascade may require investigating the interplay between ROS and the transthylakoidal proton gradient, which has been identified as a key driver of photobehavior [65]. In parallel, the interaction between ROS and intracellular calcium signaling also should be explored, as both are central components of microalgal adaptation to environmental stressors such as high irradiance [12, 23, 64, 66–70]. Notably, calcium has already been identified as essential to the phototactic behavior in benthic diatoms [17, 18, 71, 72]. Moreover, it could be interesting to explore the role of oxidized metabolites, particularly oxylipins produced through direct lipid-peroxidation, some of which act as infochemicals [9] and secondary messengers [66, 73].

SYNERGY BETWEEN MIGRATION, PIGMENT CONTENT AND PHOTOPHYSIOLOGICAL STATE

To complement the experimental results that showed MPB vertical migration behavior was mediated, at least in part, by ROS, the metabolic cost associated with oxidative stress was assessed through key photosynthetic parameters and pigment responses in both SB and WSB groups.

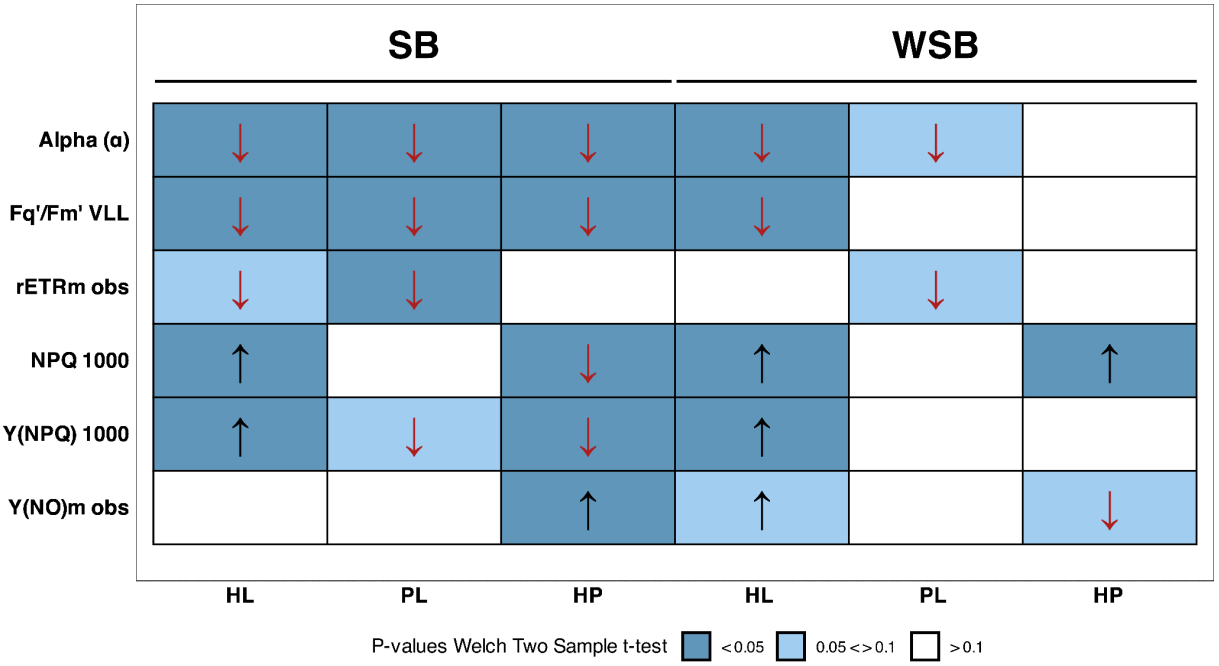

Figure 3. Heatmap of net photophysiological responses under oxidative stresses.

Net impact of High Light (HL), Hydrogen Peroxide (HP), and Cold Atmospheric Plasma (PL) stress on photosynthetic parameters. Welch's two-sample t-test (n = 3) was used to calculate the stress-induced changes (Δ After − Before) relative to the Very Low Light-adapted control (Δ After − Before VLL), in order to correct for the natural photophysiological variation observed under VLL conditions. Arrows indicate the direction of the change induced by each stressor compared to the VLL control. α (arbitrary units) refers to the maximum light use coefficient for PSII at low light. Fq'/Fm'_{VLL} (unitless) corresponds to the maximum quantum yield of PSII in the VLL-adapted state. $rETR_{m\ obs}$ (arbitrary units) and $Y(NO)_{m\ obs}$ (unitless) refer to the maximum values observed within the measured light curve range (without extrapolation). NPQ^{1000} (unitless) and $Y(NPQ)^{1000}$ (unitless) correspond to the values observed at the highest light step of the light curve (without extrapolation). All fluorescence measurements were performed on VLL-adapted samples for both Sediment Biofilm (SB) and Without Sediment Biofilm (WSB) sample groups. See Table S3 for detailed values.

Photophysiological response. Photosynthetic parameters derived from Chla fluorescence are reliable indicators of cellular physiological state under various abiotic stresses [74]. However, in vertically migrating microphytobenthic communities, such data should be interpreted with caution [46, 75, 76]. SB group results highlighted a general decrease in photosynthetic efficiency under all three stresses, characterized by a drop in α, Fq'/Fm'_{VLL}, $rETR_{m\ obs}$, indicating that vertical migration did not maintain photosynthetic performances in the short term, as previously shown by Prins et al. (2020) and Morelle et al. (2025) [24, 56]. A photoprotective response was observed only under HL, with increased NPQ^{1000} and $Y(NPQ)^{1000}$, indicating controlled dissipation of excess energy (**Figure. 3**; detailed values provided in **Table. S3**). These results are influenced by a combination of factors associated with the presence of sediment, which allowed favorable orientation of diatom cells, attenuated the light perceived during the light curve program and enabled downward migration under the three stress conditions, potentially leaving less viable cells at the surface [76]. Additionally,

interactions between exogenous ROS, notably H_2O_2 from HP and PL stress, and dissolved organic matter in the sediment may have promoted the formation of more reactive and toxic radicals such as $HO^{\bullet}$, further contributing to unfavorable conditions [77].

The WSB group mitigates these biases, providing a clear interpretation of the physiological impact on MPB cells. Exposure to stress in the absence of sediment, and thus any possibility for vertical migration, revealed a marked photophysiological impact under HL, with photoprotection activation similar to SB group, as well as a trend toward increased unregulated photoinhibition, as indicated by $Y(NO)_{m\ obs}$ (**Figure. 3**). Conversely, HP and PL did not significantly alter the state of the photosynthetic electron transport chain, indicating that these stresses remained within physiologically acceptable limits for the cells, despite their inability to migrate. This lack of impact is especially noticeable when comparing the response curves of Fq'/Fm', Y(NPQ) and Y(NO) (**Figure. 4**).

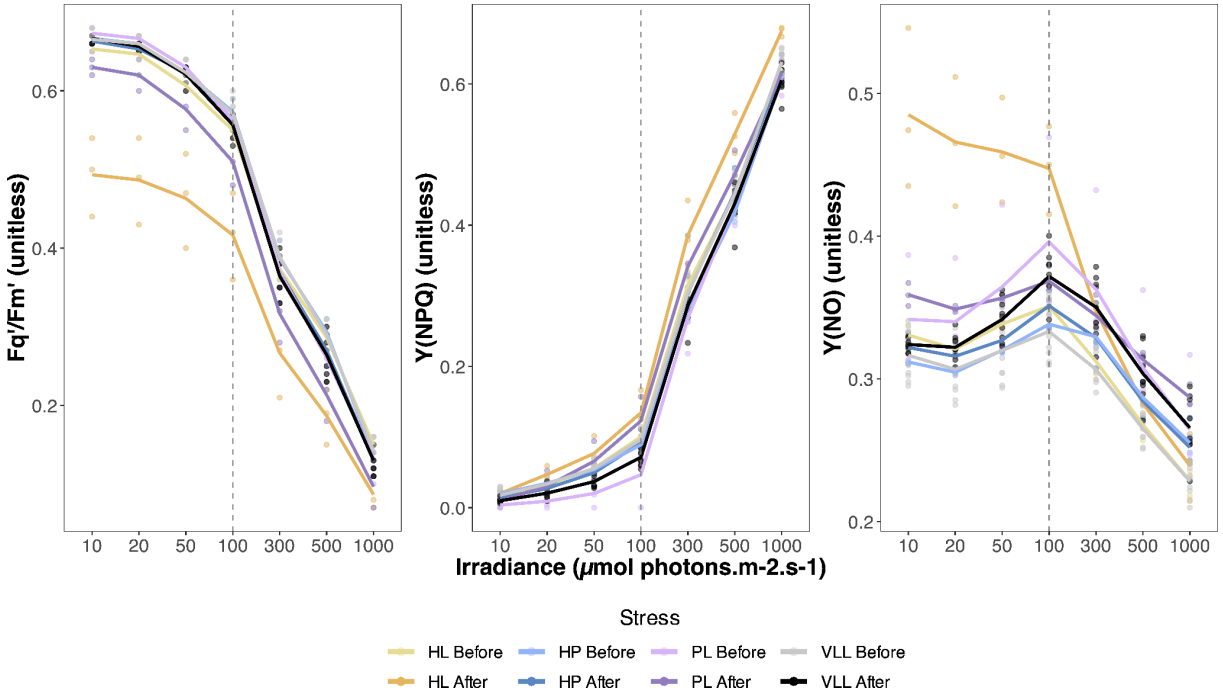

Figure 4. Stress-induced photosynthetic efficiency profiles in the WSB group

Unitless Fq'/Fm', Y(NPQ), and Y(NO) response curves of Without Sediment Biofilm (WSB) group samples under the three stress conditions: High Light (HL), Hydrogen Peroxide (HP) and Cold Atmospheric Plasma (PL), compared to the Very Low Light (VLL) adapted control. All photosynthetic parameters measured with n = 3.

All response curves, both before and after stresses, exhibited similar profiles. Notably, a shift in photosynthetic dynamics was observed between 100 and 300 µmol photons m^{-2} s^{-1}, characterized by an initial increase in Y(NO) up to this threshold, followed by a reversal of the trend and a subsequent decrease. At the same time, a continuous increase in regulated non-photochemical quenching Y(NPQ) and a decline in Fq'/Fm' were observed. The only difference in curve profiles was observed under HL, with significantly lower Fq'/Fm' values after stress, right from the lowest irradiances, indicating

damage to PSII and resulting in an increase in Y(NO). It is important to note that HL did not compromise the capacity of the functional PSII to perform Y(NPQ).

The results highlight a difference between the pathways involved in vertical migration and those driving the photophysiological response, with the strongest downward migration observed under stresses that had the least impact on photosynthesis.

General pigment response. The analysis of MPB lipophilic pigments revealed a composition dominated by the three major diatom pigments : Chlorophyll *a*, Fucoxanthin and Chlorophyll *c2*, along with their derivatives (**Fig. S6**). It also highlighted a broader diversity of the autotrophic community, less apparent in the metabarcoding results, through the detection of the VAZ cycle, Lutein, and Neoxanthin [26].

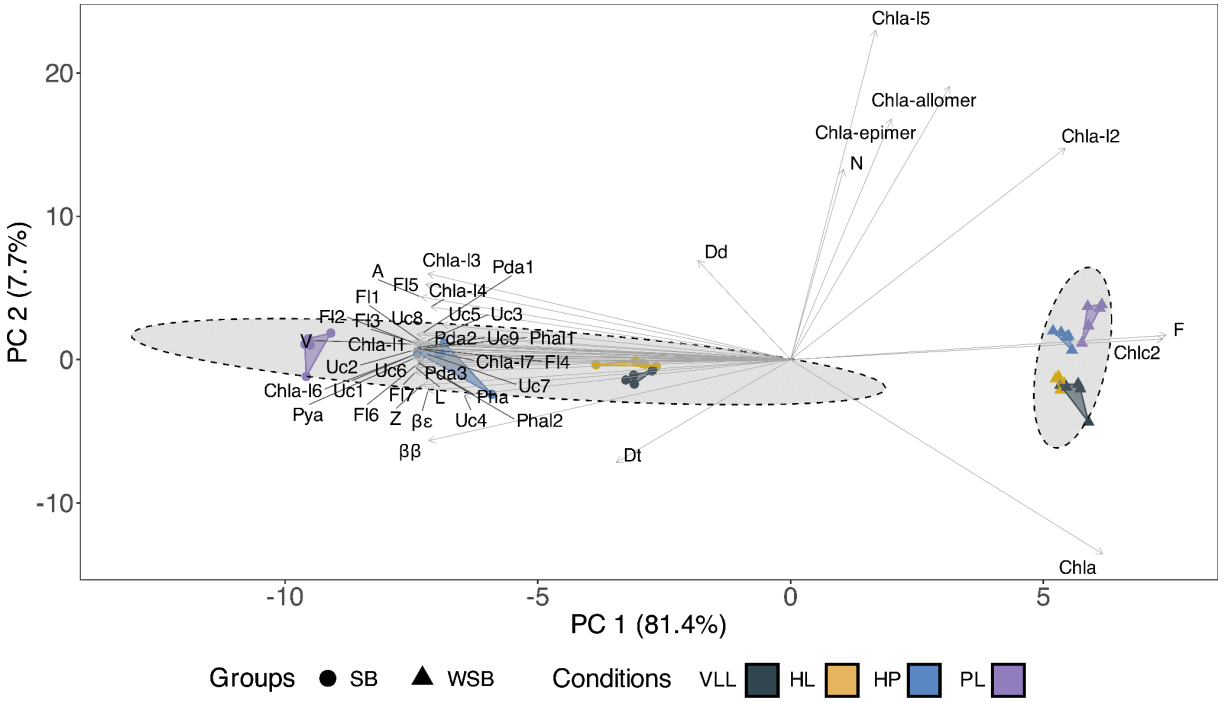

Figure 5. Pigment composition of SB and WSB under oxidative stress

Biplot of relative pigment abundances and the projection of pigment variables onto the first two principal components (PC1 and PC2) from the PCA. Samples are grouped by Sediment Biofilm (SB) and Without Sediment Biofilm (WSB) groups, under different conditions: Very Low Light adapted control (VLL), High Light (HL), Hydrogen Peroxide (HP), and Cold Atmospheric Plasma (PL). Dashed lines indicate 95% confidence ellipses and pigments abbreviations are provided in Table. S2.

SB and WSB samples were characterized by a clear difference in their pigment compositions (ANOSIM, R = 1; p-value = 1e-04, performed on individual PCA coordinates), with significant differences in the relative proportions of all pigments except for Dd (SIMPER, p-value = 0.06). WSB

samples showed higher relative proportions of Chla, Fucoxanthin, and Chlorophyll *c2*, whereas SB samples exhibited increased relative proportions of degraded pigments such as Pheopigments, Unknown Carotenoids, or Fucoxanthin-like (**Figures. 5 and S6**). The experimental protocol could lead to autoxidation artifacts [78–81]. Nevertheless, the enrichment in Chla-derivatives and Pheopigments in VLL SB clearly indicated the presence of extracellular pigments undergoing degradation within the biofilm matrix and sediment, compared to sediment-deprived VLL WSB. Moreover, the degraded forms also result from the significant impact of stress on pigments (ANOSIM R = 0.89, p-value = 1e-04 and R = 0.91, p-value = 1e-04), which explain 84% and 66% of the total inertia of composition in the SB and WSB groups, respectively (**Fig. S7**). The higher score observed for SB likely results both from the presence of a native oxidized extracellular sedimentary pigment pool [82] and a stronger impact of HP and PL stresses, which probably interacted with the sedimentary organic matter, creating an even greater oxidative stress compared to the WSB group [77]. The higher impact of these exogenous stresses was highlighted through the analysis of transformed pigment data (%), which revealed a greater number of significantly affected pigments under PL and HP than under HL compared to VLL (SIMPER, p-value < 0.05), across both SB and WSB groups (**Fig. S8**). This gradual impact of these stressors (**Fig. S9**) was mainly driven by Chla-derivatives rather than pheopigments (**Figure. 6A and B**), suggesting a random and direct oxidation of Chla, mainly on the lateral chains [83]. Some of these alternative forms may have cellular roles depending on environmental conditions, such as modifying the absorption spectrum [84], being an integral part of photosystem I [85], or contributing to ROS detoxification under environmental stressors such as heat, acidity, temperature fluctuations, limitations in nutrients, and irradiance, although Chla-tetrapyrroles are also a source of ROS under high light conditions [6, 27, 83, 86]. The increase in these cellular Chla-derivatives could serve as an indicator of environmental stress, particularly in situations leading to elevated cellular ROS production [38].

Stressors gradually affected the pigmentary system and highlighted the strongly oxidative nature of the exogenous stresses, complementing migration findings that emphasized the necessity for rapid and substantial MPB motility under these highly oxidative and harmful environmental conditions. However, although migration response and pigment impact generally aligned, it should be noted that this was not the case for all pigments, notably the activation of xanthophylls, which corresponded more closely to the photophysiological results.

Xanthophyll cycles activation. In fact, irradiance represented a targeted stress that induced finely tuned and metabolically controlled cellular adjustments, involving subtle pigment remodeling as part of a photoprotective strategy, which works in synergy with vertical migration behavior (**Fig.**

S10). Alongside a significant increase in NPQ^{1000}, the MPB community under HL exhibited activation of XC for both D-DES and Z-DES, particularly in WSB where the average de-epoxidation rates exceeded 45% and 25%, respectively (**Fig. 6C and D**; concentrations detailed in **Table. S4**).

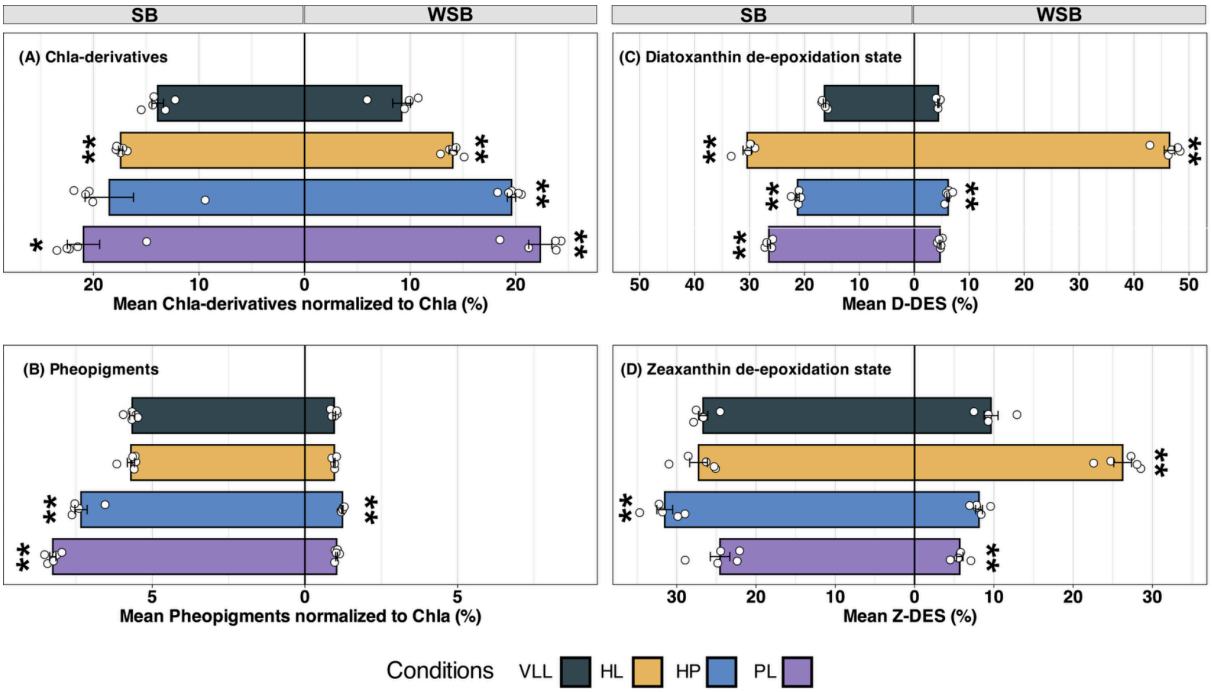

Figure 6. Impact of conditions on pigment content
*Barplot of the variation in different pigment ratios (%), under different conditions: Very Low Light adapted control (VLL), High Light (HL), Hydrogen Peroxide (HP), and Cold Atmospheric Plasma (PL), for both Sediment Biofilm (SB) and Without Sediment Biofilm (WSB) sample groups. Statistical differences are assessed by the Mann–Whitney U test between VLL and each stresses (n=5, p-value < 0.05 * ; < 0.01 **).* ***(A)*** *Barplots of the pigment ratio of Chla-derivatives concentrations.* ***(B)*** *Barplots of the pigment ratio of Pheopigments concentrations.* ***(C)*** *Barplots of the de-epoxidation state D-DES (%).* ***(D)*** *Barplots of the de-epoxidation state Z-DES (%). See Table S4 for detailed pigment concentration values.*

In contrast to Dd and Dt, VAZ pigment concentrations remained very low, ranging from 0.3% to 2.2% of total pigments. This suggests a microalgal origin distinct from the dominant *P. strigosum* biovolume, as this photoprotective pathway, though functionally documented in *Phaeodactylum tricornutum* [87, 88], is not widely reported among other benthic diatoms. HL induces rapid and efficient thermal energy dissipation, supported by the Dd + Dt xanthophyll pool size, as overstimulation of the photosynthetic electron transport chain leads to lumen acidification, which upregulates de-epoxidase enzyme activity sensitive to minimal pH variations [12, 29, 89, 90]. In addition to NPQ, carotenoid accumulation may contribute to intracellular ROS detoxification through direct scavenging enabled by molecular double bonds and polyene chains [12, 27, 30, 87, 91–93]. Furthermore, *de novo* synthesis of xanthophylls may occur, resulting in their accumulation within the thylakoid lipid membrane, where they form a lipid shield near the Fucoxanthin-Chlorophyll-Proteins

[28, 94]. The inability to adjust cellular orientation and perform vertical migration in WSB was compensated by a stronger XC activation under photooxidative stress, a well-documented photoprotective mechanism in microalgae to limit intracellular ROS accumulation [11, 12, 30, 87, 92], which explains the difference observed with SB, in addition to the reduction of light conditions induced by the presence of sediment. Similar to the WSB group, light treatment combined with latrunculin motility inhibitors [20] further underscores the importance of vertical migration by revealing comparable results on XC engagement [24, 95, 96]. In natural environments, this synergy is evident when comparing D-DES activation in epipsammic diatoms, which inhabit brighter environments where vertical migration is less effective, resulting in a stronger response than in epipelic diatoms [95, 97, 98].

Regarding exogenous ROS, it is interesting to note that despite the short duration of the applied stresses, a significant increase in NPQ^{1000} was observed, along with a slight rise in D-DES under HP WSB, whereas no such response was detected under PL, possibly due to its short duration or insufficient intensity. Flori et al. (2025) [70] report that the addition of 100 µM exogenous H_2O_2 for 30 minutes leads to its stromal accumulation, resulting in a transient decrease in PSII efficiency and a significant increase in NPQ after 60 minutes. This xanthophyll activation may result from an interplay between ROS and pathways regulating redox homeostasis and intracellular pH, which modulate de-epoxidation activity [28]. Full NPQ induction requires several components, and Dt accumulation alone does not always contribute to this process [90, 94, 99, 100]. The lack of NPQ^{1000} increase in HP and PL SB, despite XC activation, suggests that ROS may have triggered xanthophyll biosynthetic pathways for their direct use as antioxidants [12, 18, 28], or alternatively, that vertical migration masked NPQ.

All the elements presented here highlight the key signaling role of ROS, notably H_2O_2, in triggering and driving the rapid and plastic vertical migration behavior of diatom-dominated microphytobenthic biofilms, regardless of the applied stress. The variable intensity of the migration response, depending on the characteristics of oxidative stress, differentially affected the pigmentary system and highlighted a distinction between the pathways involved in vertical migration and those underlying the photophysiological response. Exogenous hydrogen peroxide and PL-ROS induced broad oxidative stress that required rapid and substantial motility in MPB to mitigate cellular damage. In contrast, irradiance triggered a more targeted and regulated response, characterized by the activation of the xanthophyll cycle, which operated synergistically with the migration strategy. Notably, when vertical migration was impaired, xanthophyll cycle activity increased, compensating for the reduced mobility. Together, these results indicate that vertical migration enables benthic diatoms to mitigate

ROS-induced cellular stress, thereby maintaining cellular homeostasis and supporting long-term physiological efficiency.

Overall, these findings provide evidence of the importance of ROS-mediated cellular signaling in shaping microphytobenthos motility behavior, demonstrating that microphytobenthic diatoms can monitor both metabolic and environmental ROS. This offers new insights into the role of oxidative stress in regulating autotrophic life, particularly within the dynamic intertidal irradiance environment and on a broader scale, highlighting its impact on the functioning of the aquatic microbiome. The response to oxidative challenges is likely complex and involves a signaling cascade that requires further in-depth investigation to identify additional cellular components and fully elucidate the signal transduction pathways underlying this behavior to cope with ROS.

ACKNOWLEDGMENTS

Our thanks go to Johann Lavaud for his valuable discussions on photophysiology. We are also thankful to Manon Leroux for her essential assistance in the laboratory during the experiment.

CONFLICTS OF INTEREST

The authors declare no conflict of interest.

FUNDING

This work was funded by the Institut de l'Océan from the Sorbonne University alliance and the Muséum national d'Histoire naturelle.

DATA AVAILABILITY

All scripts used to generate the figures and perform the analyses are available on GitHub: https://github.com/adesparmet/ROS-Driven-Diatom-Biofilm-Migration, and are also archived on Zenodo: https://doi.org/10.5281/zenodo.15848440. The datasets generated and analysed during the current study are available in the Zenodo repository at https://doi.org/10.5281/zenodo.15835853. The raw sequencing data have been deposited in the European Nucleotide Archive (ENA) under project accession number **ERA33152396** (Experiments **ERX14500286 – ERX14500369**; Runs **ERR15095684 – ERR15095767**) and can be accessed via the ENA portal at https://www.ebi.ac.uk/ena/browser/view/ERA33152396. The raw chromatogram files used for pigment analyses are available in the Zenodo repository at https://doi.org/10.5281/zenodo.15847025.

AUTHOR CONTRIBUTIONS

AD: Conceptualization, Methodology, Investigation, Data curation, Formal analysis, Visualization, Writing - original draft. BJ: Data curation, Formal analysis, Validation, Writing - review & editing. TR: Data curation, Methodology, Formal analysis. TD: Resources, Methodology, Writing - review & editing. CH: Supervision, Methodology, Data curation, Formal analysis, Validation, Writing - review & editing.

REFERENCES

1. Kühl M, Jorgensen BB. The light field of microbenthic communities: Radiance distribution and microscale optics of sandy coastal sediments. *Limnol Oceanogr* 1994;**39**:1368–1398. https://doi.org/10.4319/lo.1994.39.6.1368
2. Underwood GJC. Microphytobenthos. Encyclopedia of Ocean Sciences. Elsevier, 2001, 1770–1777.
3. Pinckney JL. A Mini-Review of the Contribution of Benthic Microalgae to the Ecology of the Continental Shelf in the South Atlantic Bight. *Estuaries and Coasts* 2018;**41**:2070–2078. https://doi.org/10.1007/s12237-018-0401-z
4. Hubas C, Passarelli C, Paterson DM. Microphytobenthic Biofilms: Composition and Interactions. In: Beninger PG (ed.), Mudflat Ecology. Cham: Springer International Publishing, 2018, 63–90.
5. Lepetit B, Dietzel L. Light signaling in photosynthetic eukaryotes with 'green' and 'red' chloroplasts. *Environmental and Experimental Botany* 2015;**114**:30–47. https://doi.org/10.1016/j.envexpbot.2014.07.007
6. Foyer CH, Hanke G. ROS production and signalling in chloroplasts: cornerstones and evolving concepts. *The Plant Journal* 2022;**111**:642–661. https://doi.org/10.1111/tpj.15856
7. Doose C et al. Non-enzymatic oxylipin production in a mudflat microphytobenthic biofilm: evidence of a diatom response to light. *Front Photobiol* 2024;**2**:1441713. https://doi.org/10.3389/fphbi.2024.1441713
8. Nishiyama Y, Allakhverdiev SI, Murata N. A new paradigm for the action of reactive oxygen species in the photoinhibition of photosystem II. *Biochimica et Biophysica Acta* 2006;**1757**:742–749. https://doi.org/10.1016/j.bbabio.2006.05.013
9. Knieper M, Viehhauser A, Dietz K-J. Oxylipins and Reactive Carbonyls as Regulators of the Plant Redox and Reactive Oxygen Species Network under Stress. *Antioxidants* 2023;**12**:814. https://doi.org/10.3390/antiox12040814
10. Mittler R et al. ROS signaling: the new wave? *Trends in Plant Science* 2011;**16**:300–309. https://doi.org/10.1016/j.tplants.2011.03.007

11. Serôdio J et al. Efficiency of photoprotection in microphytobenthos: role of vertical migration and the xanthophyll cycle against photoinhibition. *Aquat Microb Ecol* 2012. https://doi.org/10.3354/ame01591
12. Blommaert L. Photoprotection in intertidal benthic diatoms. 2017;**Ph.D. dissertation. Ghent University. Faculty of Sciences, Ghent, Belgium.**
13. Fauvel P, Bohn G. Le rythme des marées chez les diatomées littorales. CR Séanc. Soc. Biol, 1907.
14. Consalvey M, Paterson DM, Underwood GJC. THE UPS AND DOWNS OF LIFE IN A BENTHIC BIOFILM: MIGRATION OF BENTHIC DIATOMS. *Diatom Research* 2004;**19**:181–202. https://doi.org/10.1080/0269249X.2004.9705870
15. Coelho H, Vieira S, Serôdio J. Endogenous versus environmental control of vertical migration by intertidal benthic microalgae. *European Journal of Phycology* 2011;**46**:271–281. https://doi.org/10.1080/09670262.2011.598242
16. Barnett A et al. The Vertical Migratory Rhythm of Intertidal Microphytobenthos in Sediment Depends on the Light Photoperiod, Intensity, and Spectrum: Evidence for a Positive Effect of Blue Wavelengths. *Front Mar Sci* 2020;**7**:212. https://doi.org/10.3389/fmars.2020.00212
17. Cohn S, Manoylov K, Gordon R (eds). Diatom Gliding Motility. John Wiley & Sons, 2021.
18. Serôdio J. Diatom Motility: Mechanisms, Control and Adaptive Value. In: Cohn S, Manoylov K, Gordon R (eds.), Diatom Gliding Motility, 1st ed. Wiley, 2021, 159–183.
19. Morelle J et al. The Photoprotective Behavior of a Motile Benthic Diatom as Elucidated from the Interplay Between Cell Motility and Physiological Responses to a Light Microgradient Using a Novel Experimental Setup. *Microb Ecol* 2024;**87**:40. https://doi.org/10.1007/s00248-024-02354-7
20. Poulsen NC et al. Diatom gliding is the result of an actin-myosin motility system. *Cell Motil Cytoskeleton* 1999;**44**:23–33. https://doi.org/10.1002/(SICI)1097-0169(199909)44:1<23::AID-CM2>3.0.CO;2-D
21. Perkins R et al. Vertical cell movement is a primary response of intertidal benthic biofilms to increasing light dose. *Mar Ecol Prog Ser* 2010;**416**:93–103. https://doi.org/10.3354/meps08787
22. Marques Da Silva J, Duarte B, Utkin AB. Travelling Expenses: The Energy Cost of Diel Vertical Migrations of Epipelic Microphytobenthos. *Front Mar Sci* 2020;**7**:433. https://doi.org/10.3389/fmars.2020.00433
23. Suzuki S et al. Rapid transcriptomic and physiological changes in the freshwater pennate diatom *Mayamaea pseudoterrestris* in response to copper exposure. *DNA Research* 2022;**29**:dsac037. https://doi.org/10.1093/dnares/dsac037
24. Morelle J et al. Inter-specific variability in photophysiological responses of epipelic diatoms to the actin inhibitor Latrunculin B. *Diatom Research* 2025;1–14. https://doi.org/10.1080/0269249X.2024.2447333

25. Nakov T, Beaulieu JM, Alverson AJ. Accelerated diversification is related to life history and locomotion in a hyperdiverse lineage of microbial eukaryotes (Diatoms, Bacillariophyta). *New Phytologist* 2018;**219**:462–473. https://doi.org/10.1111/nph.15137
26. Roy S et al. (eds). Phytoplankton Pigments: Characterization, Chemotaxonomy and Applications in Oceanography, 1st ed. Cambridge University Press, 2011.
27. Kuczynska P, Jemiola-Rzeminska M, Strzalka K. Photosynthetic Pigments in Diatoms. *Marine Drugs* 2015;**13**:5847–5881. https://doi.org/10.3390/md13095847
28. Lepetit B et al. Photosynthetic Light Reactions in Diatoms. II. The Dynamic Regulation of the Various Light Reactions. In: Falciatore A, Mock T (eds.), The Molecular Life of Diatoms. Cham: Springer International Publishing, 2022, 423–464.
29. Goss R, Jakob T. Regulation and function of xanthophyll cycle-dependent photoprotection in algae. *Photosynth Res* 2010;**106**:103–122. https://doi.org/10.1007/s11120-010-9536-x
30. Latowski D, Kuczyńska P, Strzałka K. Xanthophyll cycle – a mechanism protecting plants against oxidative stress. *Redox Report* 2011;**16**:78–90. https://doi.org/10.1179/174329211X13020951739938
31. Furukawa T, Watanabe M, Shihira-Ishikawa I. Green- and blue-light-mediated chloroplast migration in the centric diatomPleurosira laevis. *Protoplasma* 1998;**203**:214–220. https://doi.org/10.1007/BF01279479
32. Jönsson B, Sundbäck K, Nilsson C. An upright life-form of an epipelic motile diatom: on the behaviour of *Gyrosigma balticum*. *European Journal of Phycology* 1994;**29**:11–15. https://doi.org/10.1080/09670269400650421
33. Jesus B et al. Microscale imaging sheds light on species-specific strategies for photo-regulation and photo-acclimation of microphytobenthic diatoms. *Environmental Microbiology* 2023;**25**:3087–3103. https://doi.org/10.1111/1462-2920.16499
34. De Tommasi E et al. Multiple-pathways light modulation in Pleurosigma strigosum bi-raphid diatom. *Sci Rep* 2024;**14**:6476. https://doi.org/10.1038/s41598-024-56206-y
35. Jaubert M et al. Sensing and Signalling in Diatom Responses to Abiotic Cues. In: Falciatore A, Mock T (eds.), The Molecular Life of Diatoms. Cham: Springer International Publishing, 2022, 607–639.
36. Duchêne C et al. Diatom phytochromes integrate the underwater light spectrum to sense depth. *Nature* 2025;**637**:691–697. https://doi.org/10.1038/s41586-024-08301-3
37. Nymark M et al. An Integrated Analysis of Molecular Acclimation to High Light in the Marine Diatom Phaeodactylum tricornutum. *PLoS ONE* 2009;**4**:e7743. https://doi.org/10.1371/journal.pone.0007743
38. Sachdev S et al. Abiotic Stress and Reactive Oxygen Species: Generation, Signaling, and Defense

Mechanisms. *Antioxidants* 2021;**10**:277. https://doi.org/10.3390/antiox10020277

39. Falciatore A, Mock T (eds). The Molecular Life of Diatoms. Cham: Springer International Publishing, 2022.
40. Thompson TP et al. Biomedical Application of Cold Plasma: Navigating Through Plasma Types and Devices by Antimicrobial Effectiveness and Tissue Tolerance. *Advanced Therapeutics* 2025;2400339. https://doi.org/10.1002/adtp.202400339
41. Huse SM et al. Exploring Microbial Diversity and Taxonomy Using SSU rRNA Hypervariable Tag Sequencing. *PLoS Genet* 2008;**4**:e1000255. https://doi.org/10.1371/journal.pgen.1000255
42. Caporaso JG et al. Global patterns of 16S rRNA diversity at a depth of millions of sequences per sample. *Proc Natl Acad Sci USA* 2011;**108**:4516–4522. https://doi.org/10.1073/pnas.1000080107
43. Stoeck T et al. Multiple marker parallel tag environmental DNA sequencing reveals a highly complex eukaryotic community in marine anoxic water. *Molecular Ecology* 2010;**19**:21–31. https://doi.org/10.1111/j.1365-294X.2009.04480.x
44. Eilers PHC, Peeters JCH. A model for the relationship between light intensity and the rate of photosynthesis in phytoplankton. *Ecological Modelling* 1988;**42**:199–215. https://doi.org/10.1016/0304-3800(88)90057-9
45. Silsbe GM, Kromkamp JC. Modeling the irradiance dependency of the quantum efficiency of photosynthesis. *Limnology & Ocean Methods* 2012;**10**:645–652. https://doi.org/10.4319/lom.2012.10.645
46. Consalvey M et al. PAM FLUORESCENCE: A BEGINNERS GUIDE FOR BENTHIC DIATOMISTS. *Diatom Research* 2005;**20**:1–22. https://doi.org/10.1080/0269249X.2005.9705619
47. Brotas V, Plante-Cuny M-R. The use of HPLC pigment analysis to study microphytobenthos communities. *Acta Oecologica* 2003;vol. 24, pp. S109-S115. https://doi.org/10.1016/S1146-609X(03)00013-4
48. Van Der Loos LM, Nijland R. Biases in bulk: DNA metabarcoding of marine communities and the methodology involved. *Molecular Ecology* 2021;**30**:3270–3288. https://doi.org/10.1111/mec.15592
49. Gaubert-Boussarie J, Prado S, Hubas C. An Untargeted Metabolomic Approach for Microphytobenthic Biofilms in Intertidal Mudflats. *Front Mar Sci* 2020;**7**:250. https://doi.org/10.3389/fmars.2020.00250
50. Underwood GJC, Barnett, M (eds). What determines species composition in microphytobenthic biofilms. Functioning of microphytobenthos in estuaries. Amsterdam: Royal Netherlands Academy of Arts and Sciences, 2006.
51. Méléder V et al. Spatiotemporal changes in microphytobenthos assemblages in a macrotidal flat (Bourgneuf Bay,France). *Journal of Phycology* 2007;**43**:1177–1190.

https://doi.org/10.1111/j.1529-8817.2007.00423.x

52. Serôdio J, Marques Da Silva J, Catarino F. NONDESTRUCTIVE TRACING OF MIGRATORY RHYTHMS OF INTERTIDAL BENTHIC MICROALGAE USING *IN VIVO* CHLOROPHYLL *A* FLUORESCENCE. *Journal of Phycology* 1997;**33**:542–553. https://doi.org/10.1111/j.0022-3646.1997.00542.x
53. Farré EM. The brown clock: circadian rhythms in stramenopiles. *Physiologia Plantarum* 2020;**169**:430–441. https://doi.org/10.1111/ppl.13104
54. Schneider RJ et al. Species-Level Variability in Extracellular Production Rates of Reactive Oxygen Species by Diatoms. *Front Chem* 2016;**4**. https://doi.org/10.3389/fchem.2016.00005
55. Du G et al. Behavioral and physiological photoresponses to light intensity by intertidal microphytobenthos. *J Ocean Limnol* 2018;**36**:293–304. https://doi.org/10.1007/s00343-017-6099-0
56. Prins A et al. Effect of Light Intensity and Light Quality on Diatom Behavioral and Physiological Photoprotection. *Front Mar Sci* 2020;**7**:203. https://doi.org/10.3389/fmars.2020.00203
57. Ault TR. Vertical migration by the marine dinoflagellate Prorocentrum triestinum maximises photosynthetic yield. *Oecologia* 2000;**125**:466–475. https://doi.org/10.1007/s004420000472
58. Hall N, Pearl H. Vertical migration patterns of phytoflagellates in relation to light and nutrient availability in a shallow microtidal estuary. *Mar Ecol Prog Ser* 2011;**425**:1–19. https://doi.org/10.3354/meps09031
59. De Carpentier F et al. How abiotic stress-induced socialization leads to the formation of massive aggregates in Chlamydomonas. *Plant Physiology* 2022;**190**:1927–1940. https://doi.org/10.1093/plphys/kiac321
60. Richter PR et al. High Light-induced Sign Change of Gravitaxis in the Flagellate Euglena gracilis is Mediated by Reactive Oxygen Species. *Acta protozoologica* 2003;**42**:197–204.
61. Kottuparambil S et al. UV-B affects photosynthesis, ROS production and motility of the freshwater flagellate, Euglena agilis Carter. *Aquatic Toxicology* 2012;**122–123**:206–213. https://doi.org/10.1016/j.aquatox.2012.06.002
62. Carrara F et al. Bistability in oxidative stress response determines the migration behavior of phytoplankton in turbulence. *Proceedings of the National Academy of Sciences* 2021;**e2005944118**. https://doi.org/10.1073/pnas.2005944118
63. Waszczak C, Carmody M, Kangasjarvi J. Reactive Oxygen Species in Plant Signaling. *Annual Review of Plant Biology* 2018;**69**:209–236. https://doi.org/10.1146/annurev- arplant- 042817040322
64. Graff Van Creveld S, Mizrachi A, Vardi A. An Ocean of Signals: Intracellular and Extracellular Signaling in Diatoms. In: Falciatore A, Mock T (eds.), The Molecular Life of Diatoms. Cham: Springer International Publishing, 2022, 641–678.
65. Morelle J et al. Light induced transthylakoidal proton gradient is a key signal driving the

downward migration of motile diatoms in sediments. *Scientific Reports* 2025;**15**. https://doi.org/10.1038/s41598-025-07737-5

66. Vardi A et al. A Stress Surveillance System Based on Calcium and Nitric Oxide in Marine Diatoms. *PLoS Biol* 2006;**4**:e60. https://doi.org/10.1371/journal.pbio.0040060
67. Edel KH et al. The Evolution of Calcium-Based Signalling in Plants. *Current Biology* 2017;**27**:R667–R679. https://doi.org/10.1016/j.cub.2017.05.020
68. Zhang X et al. ROS and calcium signaling mediated pathways involved in stress responses of the marine microalgae Dunaliella salina to enhanced UV-B radiation. *Journal of Photochemistry and Photobiology B: Biology* 2017;**173**:360–367. https://doi.org/10.1016/j.jphotobiol.2017.05.038
69. Pivato M et al. Compartment-specific Ca^{2+} imaging in the green alga *Chlamydomonas reinhardtii* reveals high light-induced chloroplast Ca^{2+} signatures. *New Phytologist* 2023;**240**:258–271. https://doi.org/10.1111/nph.19142
70. Flori S et al. Diatoms exhibit dynamic chloroplast calcium signals in response to high light and oxidative stress. *Plant Physiology* 2025;**197**:kiae591. https://doi.org/10.1093/plphys/kiae591
71. Cooksey B, Cooksey KE. Calcium is Necessary for Motility in the Diatom *Amphora coffeaeformis*. *Plant Physiol* 1980;**65**:129–131. https://doi.org/10.1104/pp.65.1.129
72. McLachlan DH et al. CALCIUM RELEASE FROM INTRACELLULAR STORES IS NECESSARY FOR THE PHOTOPHOBIC RESPONSE IN THE BENTHIC DIATOM *NAVICULA PERMINUTA* (BACILLARIOPHYCEAE). *Journal of Phycology* 2012;**48**:675–681. https://doi.org/10.1111/j.1529-8817.2012.01158.x
73. Pohnert G. Phospholipase A2 Activity Triggers the Wound-Activated Chemical Defense in the Diatom *Thalassiosira rotula*. *Plant Physiology* 2002;**129**:103–111. https://doi.org/10.1104/pp.010974
74. Kalaji HM et al. Chlorophyll a fluorescence as a tool to monitor physiological status of plants under abiotic stress conditions. *Acta Physiol Plant* 2016;**38**:102. https://doi.org/10.1007/s11738-016-2113-y
75. Perkins R et al. Can chlorophyll fluorescence be used to estimate the rate of photosynthetic electron transport within microphytobenthic biofilms? *Mar Ecol Prog Ser* 2002. https://doi.org/doi:10.3354/meps228047
76. Jesus B et al. Effects of vertical migrations by benthic microalgae on fluorescence measurements of photophysiology. *Mar Ecol Prog Ser* 2006;**315**:55–66. https://doi.org/10.3354/meps315055
77. Cheng K et al. Probing the Photochemical Formation of Hydroxyl Radical from Dissolved Organic Matter: Insights into the H_2 O_2 -Dependent Pathway. *Environ Sci Technol* 2025;**59**:2245–2256. https://doi.org/10.1021/acs.est.4c10348
78. Johnston LG, Watson WF. The allomerization of chlorophyll. *Journal of the Chemical Society*

(Resumed) 1956;1203–1212.

79. Cartaxana P, Brotas V. Effects of extraction on HPLC quantification of major pigments from benthic microalgae. *Archiv für Hydrobiologie* 2003;**157**:339–349. https://doi.org/10.1127/0003-9136/2003/0157-0339
80. Schagerl M, Künzl G. Chlorophyll a extraction from freshwater algae — a reevaluation. *Biologia* 2007;**62**:270–275. https://doi.org/10.2478/s11756-007-0048-x
81. Hashihama F et al. Light acclimation states of phytoplankton in the Southern Ocean, determined using photosynthetic pigment distribution. *Mar Biol* 2010;**157**:2263–2278. https://doi.org/10.1007/s00227-010-1494-5
82. Leavitt PR, Hodgson DA. Sedimentary Pigments. In: Smol JP et al. (eds.), Tracking Environmental Change Using Lake Sediments. Springer, Dordrecht, 2001, 295–325.
83. Amorim DS et al. Effects of cold plasma on chlorophylls, carotenoids, anthocyanins, and betalains. *Food Research International* 2023;**167**:112593. https://doi.org/10.1016/j.foodres.2023.112593
84. Ataka R et al. Determination of *N* -centered stereochemistry in N22-methylated chlorophyll- *a* derivatives and their epimer-dependent optical spectra. *Chirality* 2024;**36**:e23681. https://doi.org/10.1002/chir.23681
85. Fromme P. Photosystem I, Structure and Function. Encyclopedia of Biological Chemistry. Elsevier, 2004, 342–347.
86. Busch AWU, Montgomery BL. Interdependence of tetrapyrrole metabolism, the generation of oxidative stress and the mitigative oxidative stress response. *Redox Biology* 2015;**4**:260–271. https://doi.org/10.1016/j.redox.2015.01.010
87. Lohr M, Wilhelm C. Algae displaying the diadinoxanthin cycle also possess the violaxanthin cycle. *Proc Natl Acad Sci USA* 1999;**96**:8784–8789. https://doi.org/10.1073/pnas.96.15.8784
88. Giossi CE et al. Both major xanthophyll cycles present in nature can provide Non-Photochemical Quenching in the model diatom *Phaeodactylum tricornutum*. 2024. Plant Biology, 2024.
89. Lavaud J et al. Influence of the Diadinoxanthin Pool Size on Photoprotection in the Marine Planktonic Diatom *Phaeodactylum tricornutum*. *Plant Physiology* 2002a;**129**:1398–1406. https://doi.org/10.1104/pp.002014
90. Goss R et al. The importance of a highly active and ΔpH-regulated diatoxanthin epoxidase for the regulation of the PS II antenna function in diadinoxanthin cycle containing algae. *Journal of Plant Physiology* 2006;**163**:1008–1021. https://doi.org/10.1016/j.jplph.2005.09.008
91. Havaux M, Niyogi KK. The violaxanthin cycle protects plants from photooxidative damage by more than one mechanism. *Proc Natl Acad Sci USA* 1999;**96**:8762–8767. https://doi.org/10.1073/pnas.96.15.8762

92. Baroli I et al. Zeaxanthin Accumulation in the Absence of a Functional Xanthophyll Cycle Protects *Chlamydomonas reinhardtii* from Photooxidative Stress. *The Plant Cell* 2003;**15**:992–1008. https://doi.org/10.1105/tpc.010405
93. Schumann A et al. Investigation of the quenching efficiency of diatoxanthin in cells of Phaeodactylum tricornutum (Bacillariophyceae) with different pool sizes of xanthophyll cycle pigments. *Phycologia* 2007;**46**:113–117. https://doi.org/10.2216/06-30.1
94. Lepetit B et al. Evidence for the Existence of One Antenna-Associated, Lipid-Dissolved and Two Protein-Bound Pools of Diadinoxanthin Cycle Pigments in Diatoms. *Plant Physiology* 2010;**154**:1905–1920. https://doi.org/10.1104/pp.110.166454
95. Cartaxana P et al. Physiological versus behavioral photoprotection in intertidal epipelic and epipsammic benthic diatom communities. *Journal of Experimental Marine Biology and Ecology* 2011;**405**:120–127. https://doi.org/10.1016/j.jembe.2011.05.027
96. Cartaxana P et al. Regulation of Intertidal Microphytobenthos Photosynthesis Over a Diel Emersion Period Is Strongly Affected by Diatom Migration Patterns. *Front Microbiol* 2016;**7**. https://doi.org/10.3389/fmicb.2016.00872
97. Jesus B et al. Adaptations of microphytobenthos assemblages to sediment type and tidal position. *Continental Shelf Research* 2009;**29**:1624–1634. https://doi.org/10.1016/j.csr.2009.05.006
98. Barnett A et al. Growth form defines physiological photoprotective capacity in intertidal benthic diatoms. *The ISME Journal* 2015;**9**:32–45. https://doi.org/10.1038/ismej.2014.105
99. Lavaud J, Rousseau B, Etienne A-L. In diatoms, a transthylakoid proton gradient alone is not sufficient to induce a non-photochemical fluorescence quenching. *FEBS Letters* 2002b;**523**:163–166. https://doi.org/10.1016/S0014-5793(02)02979-4
100. Croteau D et al. Pennate diatoms make non-photochemical quenching as simple as possible but not simpler. *Nat Commun* 2025;**16**:2385. https://doi.org/10.1038/s41467-025-57298-4

SUPPLEMENTARY DATA

Supplementary material and Supplementary data.
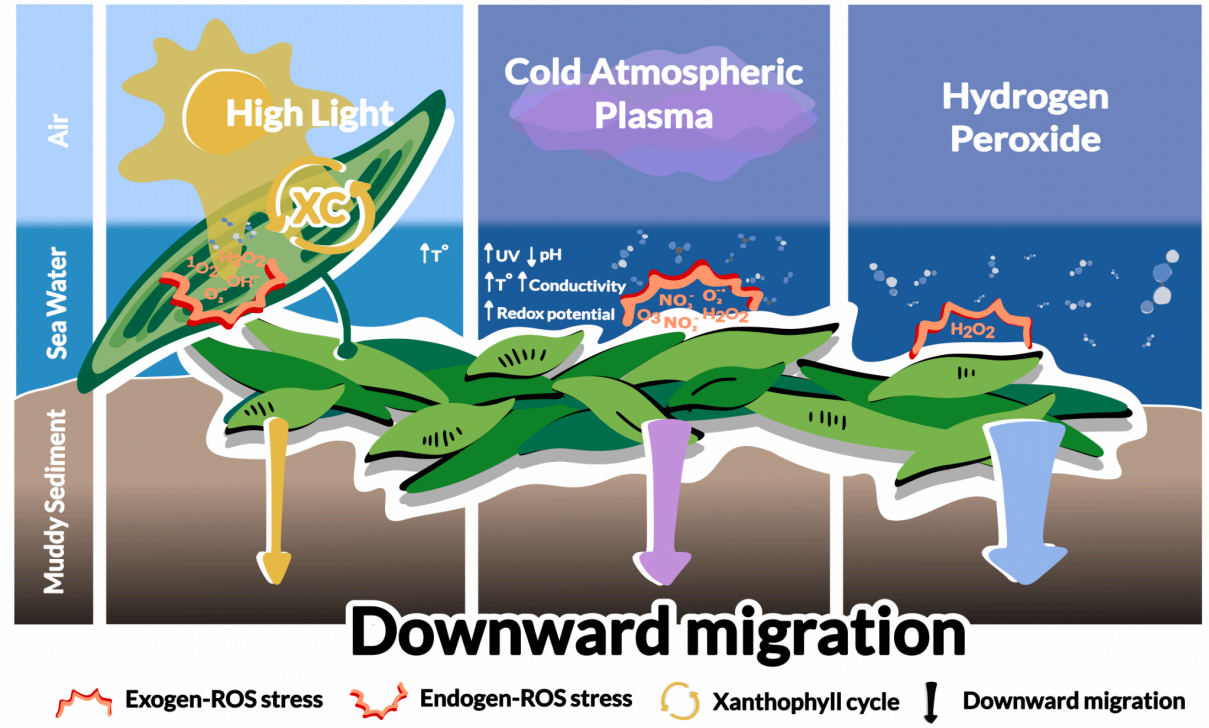
GRAPHICAL ABSTRACT